


Article

Preparation and Tribological Behaviors of Sulfur- and Phosphorus-Free Organic Friction Modifier of Amide–Ester Type

Xiaomei Xu ^{1,2}, Fan Yang ^{1,2}, Hongmei Yang ^{2,*} , Yanan Zhao ², Xiuli Sun ² and Yong Tang ²

¹ School of Materials and Chemistry, University of Shanghai for Science and Technology, Shanghai 200093, China

² State Key Laboratory of Organometallic Chemistry, Shanghai Institute of Organic Chemistry, Chinese Academy of Sciences, Shanghai 200032, China

* Correspondence: yanghm@sioc.ac.cn

Abstract: With the increasingly demanding engine conditions and the implementation of “double carbon” policies, the demand for high-quality lubricants that are cost-effective and environmentally friendly is increasing. Additives, especially high-performance friction modifiers, play an important role in boosting lubricant efficiency and fuel economy, so their developments are at the forefront of lubrication technologies. In this study, 1,3-dioleamide-2-propylolate (DOAPO), which incorporates polar amide, ester, and nonpolar alkyl chains, was synthesized from 1,3-diamino-2-propanol to give an eco-friendly organic friction modifier. Nuclear magnetic resonance (NMR), high-resolution mass spectrometry (HR-MS), Fourier-transform infrared spectroscopy (FT-IR), and thermogravimetric analysis (TGA) were used to characterize the structure and thermal stability of DOAPO. Meanwhile, the storage stability and tribological behaviors of DOAPO in synthetic base oil were studied and compared with a commercial oleamide. The results show that DOAPO has better thermal stability and better storage stability in synthetic base oil. Additionally, 0.5 wt.% of DOAPO could shorten the running-in period and reduce the average friction coefficient (ave. COF) and wear scar diameter (ave. WSD) by 8.2% and 16.2%, respectively. The worn surface analysis and theoretical calculation results show that the ester bond in DOAPO breaks preferentially during friction, which can reduce the interfacial shear force and easily react with metal surfaces to form iron oxide films, thus demonstrating a better friction-reducing and anti-wear performance.

Keywords: sulfur- and phosphorus-free; amide–ester; tribological behavior; synthetic base oil



Citation: Xu, X.; Yang, F.; Yang, H.; Zhao, Y.; Sun, X.; Tang, Y. Preparation and Tribological Behaviors of Sulfur- and Phosphorus-Free Organic Friction Modifier of Amide–Ester Type. *Lubricants* **2024**, *12*, 196.

<https://doi.org/10.3390/lubricants12060196>

Received: 31 March 2024

Revised: 27 May 2024

Accepted: 28 May 2024

Published: 30 May 2024



Copyright: © 2024 by the authors. Licensee MDPI, Basel, Switzerland. This article is an open access article distributed under the terms and conditions of the Creative Commons Attribution (CC BY) license (<https://creativecommons.org/licenses/by/4.0/>).

1. Introduction

In recent years, energy conservation and emission reduction have become one of the most urgent challenges for the automobile industry. The pursuit of improved fuel efficiency and “dual carbon” goals emphasizes the growing trend toward the use of low-viscosity oils [1], which could minimize the shear resistance between friction counterparts [2–4]. However, the shift to low-viscosity lubricants carries a certain risk of wear resistance as the lubrication regime changes from a favorable hydrodynamic lubrication to a less favorable mixed or boundary lubrication for engines with more stringent operating conditions. Under the boundary lubrication state, the lubricating films of low-viscosity oils are thin and lack of strength, resulting in direct contact and making the films break during high-strength engine operations, which would increase friction and wear [5]. Therefore, friction modifiers, which can form thick boundary films under mixed or boundary lubrication regimes, were applied to reduce or prevent direct friction solid–solid contact on friction pairs [6–8].

In general, the friction modifications used in engine oil are metal friction modifications (such as didithiophosphate zinc (ZDDP), organic molybdenum [9,10], etc.) and non-metallic friction modifications (such as oleamide [11], glycerol monooleate [3,12,13], etc.). Metal

friction improvement agents are mostly metal or metal compounds containing sulfur and phosphorus. Although they show excellent performance and are most widely used [14,15], the metal they contain will increase the ash content of lubricating oil, and the metal compounds containing sulfur and phosphorus can poison automobile catalysts used for emission control, causing adverse effects on the engine and the environment. Therefore, green non-metallic organic friction modifiers (OFMs) composed only of carbon, hydrogen, oxygen, and nitrogen atoms are attracting increasing attention [5,16,17].

OFMs tend to have amphiphilic structures, in which polar groups could adsorb onto metal surfaces, while nonpolar hydrocarbons arrange outward within the lubricant [18,19]. This arrangement establishes a hydrocarbon surface with low shear strength on metal surfaces. At present, the developed OFMs incorporate various polar functional groups, such as carboxyl [20–22], alcohol [23–25], amine [26,27], amide [5,28–30], and ester [31] functionalities. Biresaw [31] synthesized seven lipoic acid esters using various alcohols, and the study showed that the performance of thioic acid multifunctional additives in base oils is related to its structure. When the addition is 5 wt.%, 2-ethylhexyl thiocticate and dodecyl thiocticate with straight chains increased the kinematic viscosity at 40 °C from 40.8 mm²/s to 78.7 mm²/s and 69.5 mm²/s, kinematic viscosity at 100 °C from 8.7 mm²/s to 18.2 mm²/s and 15.0 mm²/s, the viscosity index from 200 to 253 and 229, showing a good viscosity improvement performance. Compared with the base oil, the addition of 20 wt.% lipoic acid ester makes the onset oxidation temperature and extreme pressure load increase from 187.2 °C to 218.4–221.5 °C, and 120 kgf to 420–480 kgf, respectively, showing a good anti-oxidation and extreme pressure performance.

Hou [5] prepared a novel organic friction modifier N-(2,2,6,6-tetramethyl-1-oxyl-4-piperidyl) dodecenamide (C₁₂Amide-TEMPO) and found it can form a unique double-layer boundary film on the iron oxide surface, i.e., the strong surface adsorption layer formed by chemical interactions between amide oxygen, free radicals, and iron oxide surfaces, as well as the interlayer hydrogen bond films formed by amide hydrogen and free radicals or oxygen. Meanwhile, the combination of intra-layer and inter-layer hydrogen bonds also increases the strength of the boundary film by enhancing cohesion, so C₁₂Amide-TEMPO is better than the traditional glyceryl monooleate (GMO) and stearic acid in terms of bearing capacity, friction reduction, and friction stability. Compared to GMO and stearic acid at an effective load of 5.0 N, C₁₂Amide-TEMPO demonstrates a more stable instantaneous friction coefficient (COF), with over 60% reduction in wear rate and surface roughness. The groove width and wear rate of wear scar lubricated with C₁₂Ester-TEMPO or C₁₂Amino-TEMPO is 569.0 μm, 544.0 μm and 461.2 μm³/(N·mm), 196.9 μm³/(N·mm), which is significantly higher than 365.0 μm and 42.2 μm³/(N·mm) that lubricated with C₁₂Amide-TEMPO. This indicates that C₁₂Amide-TEMPO with an amide-linked structure outperforms C₁₂Ester-TEMPO and C₁₂Amino-TEMPO in terms of friction-reducing and anti-wear properties. However, the long-term stability and durability study of these OFMs remains limited.

The reported studies show that ester- or amide-based compounds exhibit good performance in improving friction; however, the prepared additives are all individual esters or amides. Compared to a single-functional group, molecules with multiple functional groups would enhance adsorption strength through multi-site adsorption or chelation effects, improving the stability and durability of tribofilms and demonstrating excellent tribological performance. Additionally, most of the reported tribological properties were evaluated in PAO6, whose viscosity is relatively higher (kinematic viscosity of ~5.80 cSt at 100 °C). With increasingly stringent global emission regulations, low-viscosity lubricant technology has become a well-known trend in recent years [32], so the performance of additives should be conducted in lower-viscosity oils, such as PAO4 (kinematic viscosity of ~3.90 cSt at 100 °C). In this study, we designed and synthesized an eco-friendly OFM with a ternary structure based on amide, ester, and hydrocarbons. 1,3-diamino-2-propanol and oleic acid (OA) were used to prepare the 1,3-dioleamide-2-propylolate (DOAPO), which was characterized by NMR, HR-MS, FT-IR, and TGA. Meanwhile, the storage stability and tribological behaviors of DOAPO were investigated in a low-viscosity synthetic base oil and

compared with a commercial oleamide. Additionally, micro-IR, XPS, and DFT calculations were applied to clarify its micro-lubrication mechanism.

2. Materials and Methods

2.1. Materials

1,3-diamino-2-propanol (98%) and 4-dimethylaminopyridine (DMAP, 99%) were obtained from Beijing Innochem Co., Ltd. (Beijing, China). Oxalyl chloride (98%), N, N-dimethylformamide (DMF, 99.5%), and triethylamine (TEA, 99%) were received from Energy Chemical. Dichloromethane (DCM, Shanghai Titan Scientific Co., Ltd. (Shanghai, China), 99.9%), oleic acid (OA, Alfa Aesar Chemical Co., Ltd. (Hangzhou, China), 99%), and all other reagents were commercially obtained and used as received for the synthesis of DOAPO.

Durasyn[®]164 (PAO4, INEOS, London, UK) and Priolube 3970 (3970, CRODA, Snaith, UK) were separately purchased from Shanghai Qicheng Industrial Co., Ltd. (Shanghai, China) and Hersbit Chemical Co., Ltd. (Shanghai, China), which were applied as base oils for the tribological evaluation of DOAPO, and oleamide (Tokyo Chemical Industry Co., Ltd. (Tokyo, Japan), 65%) was used as a commercial additive to compare with DOAPO.

2.2. Synthesis of 1,3-Dioleamide-2-Propylolate (DOAPO)

OA (12.55 g, 44.44 mmol), dry DCM (20 mL), and 2–3 drops of DMF were mixed in a round-bottom flask under an Ar atmosphere, and oxalyl chloride (11.28 g, 88.88 mmol) was slowly added dropwise into the mixture at 0 °C. After that, the reaction was stirred at room temperature for 4 h until the OA was transformed completely. The excess oxalyl chloride was removed by reduced pressure to yield the oily, colorless oleoyl chloride. Subsequently, the prepared oleoyl chloride was dissolved with dry DCM (20 mL) and added dropwise into a mixture of 1,3-diamino-2-propanol (1.00 g, 11.11 mmol), TEA (4.60 g, 45.55 mmol), DMAP (0.41 g, 3.33 mmol), and dry DCM (30 mL). The mixture was refluxed at 50 °C for 2 h and quenched with water when 1,3-diamino-2-propanol was completely consumed using TLC monitoring. The organic phase was extracted with DCM, washed with saturated NaHCO₃ and NaCl solutions, and dried with anhydrous Na₂SO₄. The crude product was purified by column chromatography (eluent: $V_{(DCM)}/V_{(MeOH)} = 30/1$) to obtain 1,3-dioleamide-2-propylolate as a pale-yellow liquid (6.20 g, yield: 63%), which was recorded as DOAPO.

¹H NMR (400 MHz, CDCl₃) δ 6.22 (s, 2H), 5.34 (s, 6H), 4.83 (s, 1H), 3.49 (s, 2H), 3.30 (d, J = 14.1 Hz, 2H), 2.29 (t, J = 7.5 Hz, 2H), 2.21 (t, J = 7.5 Hz, 4H), 2.00 (d, J = 5.5 Hz, 12H), 1.63 (s, 6H), 1.28 (d, J = 14.2 Hz, 60H), 0.87 (t, J = 6.3 Hz, 9H) (Figure S1a). ¹³C NMR (101 MHz, CDCl₃) δ 174.11, 173.18, 130.19, 130.15, 129.86, 129.82, 77.48, 77.16, 76.84, 71.21, 39.13, 36.94, 34.44, 33.95, 32.06, 29.92, 29.88, 29.68, 29.48, 29.42, 29.36, 29.31, 29.29, 27.39, 27.34, 25.88, 25.02, 22.83, 14.24 (Figure S1b). HR-MS (ESI) calcd. for C₅₇H₁₀₇N₂O₄ [M+H]⁺: 883.82254, found: 883.82341 (Figure S1c). FT-IR (ATR): ν = 3292.0, 3079.6, 2922.7, 2853.3, 1739.1, 1651.7, 1548.5, 1465.0, 1377.5, 1246.1, 1172.6, 1083.8, 722.6 cm⁻¹ (Figure S1d).

2.3. Characterization

The nuclear magnetic resonance (NMR) characterization, including ¹H NMR and ¹³C NMR, was conducted on a 400-MR (Varian, Palo Alto, CA, USA) using CDCl₃ as the solution. High-resolution mass spectrometry (HR-MS) was carried out on JMS-T100LP AccuTOF LC-plus 4G (Nippon Electronics Corporation, Tokyo, Japan) using electrospray ionization. Nicolet iN10MX (Thermo Fisher, Waltham, MA, USA) was applied to record Fourier-transform infrared (FT-IR) and micro-infrared (micro-IR) spectroscopy by scanning from 400 to 4000 cm⁻¹. Thermogravimetric analysis (TGA) was performed on Q500 (TA, Milford, MA, USA) under a N₂ atmosphere with a flow rate of 60 mL/min and a heating rate of 10 °C/min from 25 to 600 °C. The morphology and elemental composition of metal surfaces are analyzed by scanning electron microscope with energy dispersive spectrometer (SEM-EDS) using QUANTAX (Bruker, San Jose, CA, USA). The chemical state of specific

elements and potential tribochemical films formed on the frictional surface were analyzed using X-ray photoelectron spectroscopy (XPS, Thermo Scientific K-Alpha, Waltham, MA, USA) with an Al-K α radiation source, and the obtained spectra were analyzed using the Advantage 5.9931 software.

2.4. Oil Preparation

In this study, the synthetic hydrocarbon PAO4 (90 wt.%) and saturated polyol ester 3970 (10 wt.%), which are both low viscosity, were blended after heating and stirring at 60 °C for 2 h to obtain the base oil. Oil samples containing additives were prepared as follows: 0.05–1.0 wt.% of self-prepared DOAPO or purchased oleamide, and the base oil was mixed at 60 °C for 2 h.

2.5. Tribological Test

The tribological behaviors of DOAPO in base oil were evaluated on a Tenkey MS-10A four-ball tester (Xiamen TenKey Automation Co., Ltd., Xiamen, China), which was compared with that of commercially available oleamide. A picture of the four-ball tester and its schematic are shown in Figure 1; all balls used are made of GCr15-bearing steel with a diameter of 12.7 mm. According to the standard NB/SH/T 0189-2017 [33], the tribological tests were operated at 75 °C for 1 h, where the rotational speed of the upper steel ball was 1200 rpm, and the load was 392 N. Each test was conducted at least three times to ensure the repeatability of the average friction coefficient (ave. COF) and average wear scar diameter (ave. WSD).

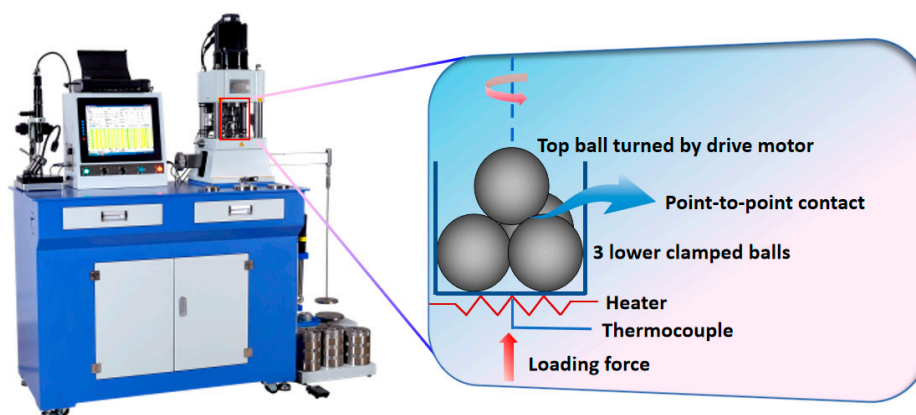
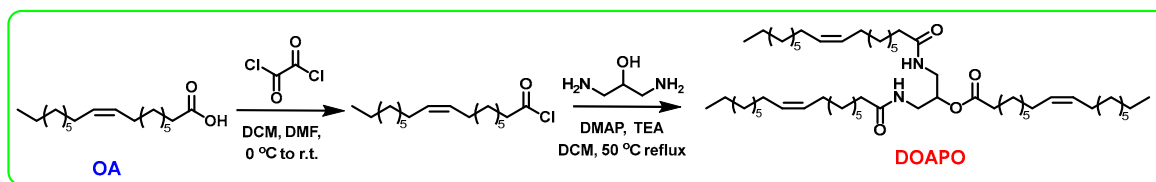


Figure 1. A picture of the MS-10A four-ball tester and its schematic.

3. Results and Discussion

3.1. Synthesis Route of DOAPO

At present, the synthesis of amides mainly includes direct amidation of carboxylic acids and amines; amidation of acyl halogens, anhydrides, or esters; hydrolysis of amides by oximes or nitriles; amidation of alcohol oxidation; and so on. Among them, the amidation of acyl halogens, namely the Schotten–Baumann reaction, is the most convenient and efficient method. Meanwhile, the reaction rate of carboxylic acid activated to acyl chloride is fast, even for substrates with large site resistance. Therefore, oxalyl chloride is used to activate OA to oleoyl chloride in this work, which can react simultaneously with the amine and hydroxyl groups of 1,3-diamino-2-propanol to obtain DOAPO; the synthesis route is shown in Scheme 1. NMR, HR-MS, and FT-IR were used to confirm the structure of DOAPO, and the results can be seen in Section 2.2.



Scheme 1. The synthesis route of DOAPO.

3.2. Thermal Stability of DOAPO

In general, high-quality lubricants such as engine oils, anti-wear hydraulic oils, compressor oils, etc., all require a good high-temperature resistance. Although the thermal stability of lubricants mainly depends on base oils, it is worth noting that many additives with lower decomposition temperatures will adversely affect the overall stability of lubricants, thus reducing their comprehensive performance and service life. So, thermal stability is a key index to estimate the effectiveness of additives. The TG and DTG curves of 1,3-diamino-2-propanol, DOAPO, and commercial oleamide are shown in Figure 2. Combining the comparison data in Table S1, the initial and terminal decomposition temperatures of 1,3-diamino-2-propanol, DOAPO, and oleamide are 58.4 °C and 188.9 °C, 495.0 °C, and 329.9 °C, respectively; their maximum decomposition temperatures are 178.1 °C, 395.5 °C, and 307.8 °C, respectively. Meanwhile, the residual masses of 1,3-diamino-2-propanol, DOAPO, and oleamide at 300 °C and 400 °C are 0.06%, 86.9%, and 33.9% and 0.02%, 20.1%, and 0.3%, respectively. The results show that the thermal stability of the three can be ranked as DOAPO > oleamide > 1,3-diamino-2-propanol. Due to the introduction of an oleacyl group with a long carbon chain, the thermal stability of DOAPO is significantly improved compared with the raw material 1,3-diamino-2-propanol, even better than that of commercial oleamide.

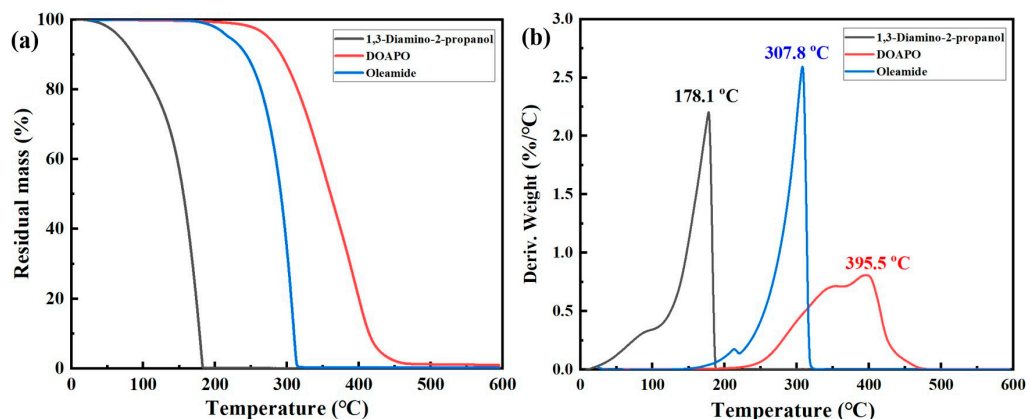


Figure 2. (a) TG and (b) DTG curves of 1,3-diamino-2-propanol, DOAPO, and oleamide.

3.3. Storage Stability of DOAPO in Synthetic Base Oil

Good storage stability is the basic requirement to ensure the performance of lubricants, which is primarily determined by the stability of additives in base oils. Therefore, we have investigated the storage stability of oils with different additions of DOAPO, as well as the same addition of DOAPO and commercial oleamide. As shown in Figure 3a and Table S1, after 30 days of storage at room temperature, the oil samples with 0.05~1.0 wt.% DOAPO remained clear and bright without any precipitation (Figure 3a), while the bottom of 0.5 wt.% oleamide appeared obvious precipitation (Figure 3b), indicating that the storage stability of DOAPO in synthetic base oil is better than that of oleamide.

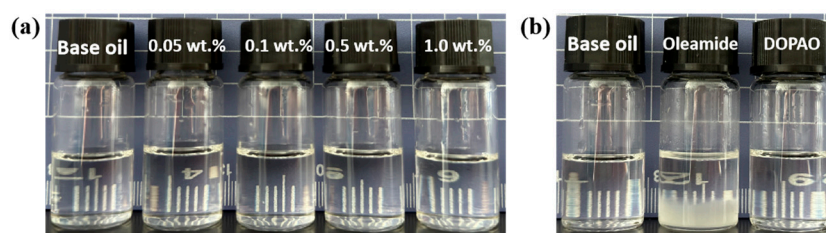


Figure 3. Appearance of oil samples after 30 d: (a) different additions of DOAPO; (b) the same addition (0.5 wt.%) of DOAPO or oleamide.

3.4. Tribological Properties of DOAPO

3.4.1. Different Additions of DOAPO

The performance of additives in base oils usually varies with different additions, exhibiting better comprehensive properties within an optimal addition range [34]. Figure 4 displays the tribological performance of oil samples with different additions of DOAPO. The friction profiles (Figure 4a) show that the running-in period of oil with a low DOAPO addition, i.e., 0.05 wt.%, is much longer than that with 0.1~1.0 wt.% (600 s vs. 120 s), which is similar to base oil. During the relative-stability period (600~3600 s), oil samples with 0.05~1.0 wt.% DOAPO are much more stable compared to base oil, even the COF of 0.05 wt.% DOAPO oil is high. It is worth noting that the COF of 0.1 wt.% DOAPO oil increases at the end of friction, which is maintained stable for 0.5 wt.% DOAPO oil. Nonetheless, the COF of 1.0 wt.% DOAPO oil fluctuates slightly in the initial phase of the relative-stability period. Overall, oils with 0.1~1.0 wt.% DOAPO exhibit better tribological properties, i.e., lower COF and smaller WSD, when compared to the base oil (Figure 4b). However, the tribological performance of 0.05 wt.% DOAPO oil is slightly worse than base oil, which may be related to the higher friction during the running-in period (see the insertion in Figure 4a). Overall, the oil with 0.5 wt.% DOAPO shows the best friction-reducing and anti-wear performance, namely reducing COF and WSD by 8.2% and 16.2% compared to base oil, respectively.

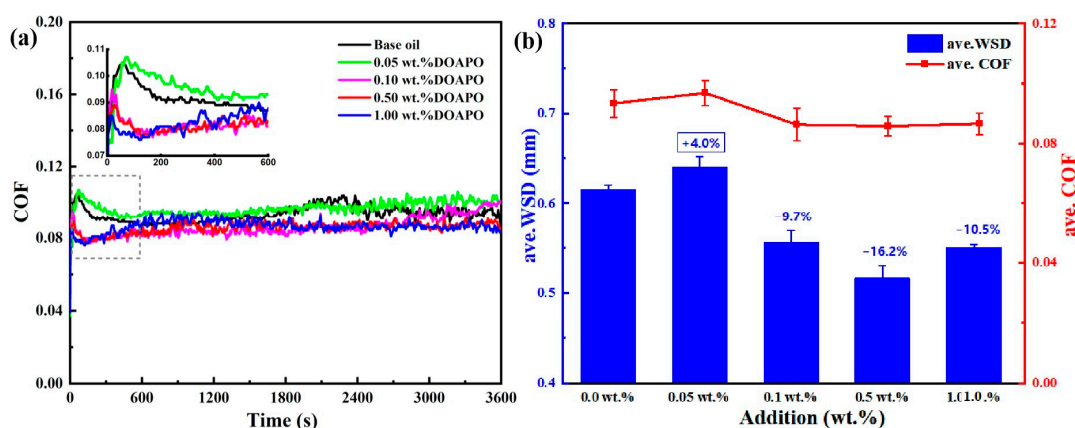


Figure 4. (a) Friction profiles and (b) ave. COF and ave. WSD of oil samples with different additions of DOAPO.

3.4.2. Comparison with the Commercial Oleamide

The tribological performance of DOAPO was compared with the commercial oleamide that has a similar structure, applying 0.5 wt.% as the optimal addition. As demonstrated in Figure 5a, both DOAPO and oleamide could shorten the running-in period to some extent when compared to the base oil, but the friction of the oil containing DOAPO is more stable. The ave. COF values during the running-in period of base oil, 0.5 wt.% DOAPO oil, and 0.5 wt.% oleamide oil are 0.094, 0.080, and 0.082, respectively. The results in Figure 5b show that oils with DOAPO and oleamide exhibit lower COF and smaller WSD than base

oil, i.e., both of them have effectiveness in friction reduction and anti-wear. Specifically, 0.5 wt.% DOAPO decreases the COF and WSD by 8.2% and 16.2%, while 0.5 wt.% oleamide decreases the COF and WSD by 2.6% and 12.0%, which indicates that the friction-reducing and anti-wear properties of DOAPO are better.

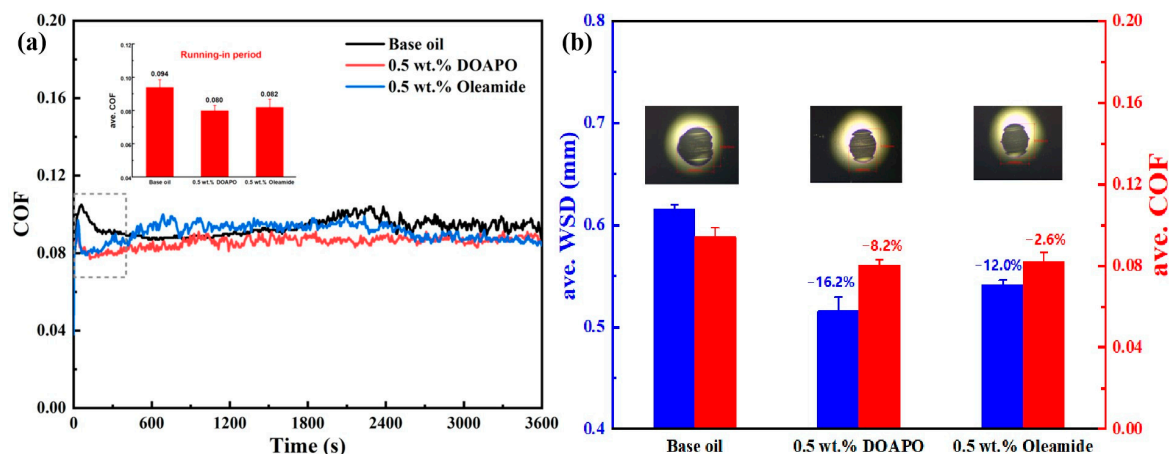


Figure 5. (a) Friction profiles and (b) ave. WSD and COF of oils with 0.5 wt.% of additives.

3.5. Micro-Lubrication Mechanism

3.5.1. Worn Surface Analysis

To investigate the micro-lubrication mechanism of the as-prepared amide-ester in synthetic base oil, micro-IR, SEM-EDS, and XPS were applied to analyze the composition of tribofilms on worn and non-worn surfaces lubricated with 0.5 wt.% DOAPO oil before and after tribological tests (marked as DOAPO_Non-wear and DOAPO_Wear, respectively), which were also compared to that with base oil (marked as Base oil_Wear). In Figure 6a, DOAPO_Non-wear not only has the stretching vibrations at 3357 cm^{-1} and 3177 cm^{-1} ($\nu_{\text{N-H}}$), bending vibration at 1632 cm^{-1} ($\delta_{\text{N-H}}$), and $\delta_{\text{C-H}}$ at 722 cm^{-1} of long alkyl chains but also has $\nu_{\text{C-O-C}}$ at 1058 cm^{-1} and 1021 cm^{-1} and $\delta_{\text{C=C-H}}$ at 892 cm^{-1} , which is characteristic for OA-based amide-ester. However, the $\nu_{\text{C-O-C}}$ at 1058 cm^{-1} and 1021 cm^{-1} and $\delta_{\text{C=C-H}}$ at 892 cm^{-1} that are characteristic of OA-based ester disappeared for DOAPO_wear, which is most likely caused by the breaking of long alkyl chain for ester in DOAPO during friction. When compared to the Base oil_Wear (Figure 6b), it has a characteristic $\nu_{\text{(CO)O-H}}$ at 1696 cm^{-1} , indicating an ester chain broken in ester 3970, which composed the base oil. According to the micro-IR results, it can be speculated that the ester group in DOAPO is more prone to be broken than the amide group when friction occurs.

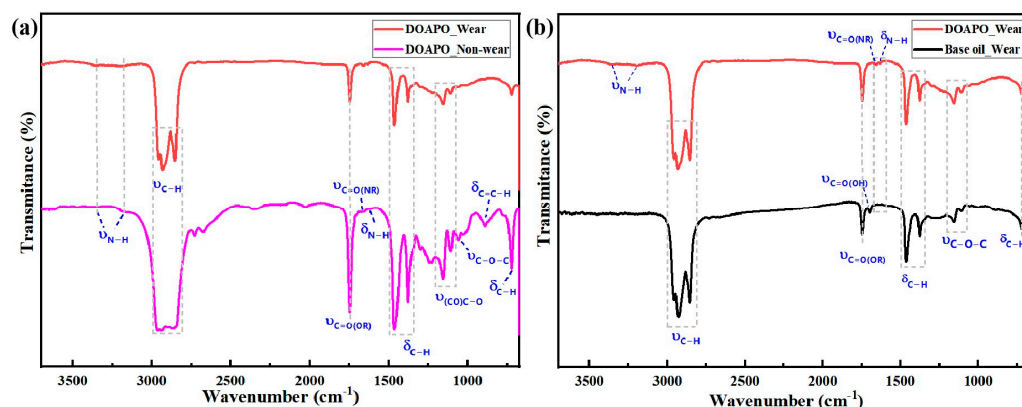


Figure 6. Micro-IR analysis of (a) worn and non-worn surfaces lubricated with 0.5 wt.% DOAPO oil and (b) worn surfaces lubricated with 0.5 wt.% DOAPO oil and base oil.

The morphology and elemental composition were analyzed by SEM-EDS, as shown in Table S3. The SEM images show that the surface wear is significantly improved when lubricated with 0.5 wt.% DOAPO. Compared with base oil, the surface lubricated with 0.5 wt.% DOAPO had lower C and slightly higher O and Fe before the tribological test, but it had higher C and Fe and lower O after the tribological test, indicating that DOAPO is involved in the formation of friction films. By further comparing the element composition of wear and non-wear surfaces lubricated with 0.5 wt.% DOAPO and base oil, it can be seen that the content of C and O for the wear surface is significantly higher than that of non-wear, and C content of surface lubricated with 0.5 wt.% DOAPO increases more, indicating that C is a key component of friction films.

XPS is mainly used to determine the binding energy of electrons. By comparing the chemical composition, bond state, and surface state before and after friction, XPS is beneficial for obtaining the chemical change information of the material surface during friction [35]. The bonding states of C, O, Fe, and N elements on worn surfaces lubricated with base oil and 0.5% DOAPO oil were further analyzed by XPS. After deconvolution (in Figure 7 and Table S4), there are three major peaks in the C1s spectra for DOAPO_Wear, i.e., C-C/C=C (284.80 eV, ~69.0%), C-O/C-N (285.94 eV, ~10.1%), and C=O (288.58 eV, ~20.90%) [36,37], whose C=O content is less than that of DOAPO_Wear. While there are only C-C/C=C (~91.6%) and C=O (~8.4%) for Base oil_Wear. In the O1s spectra, both of them have peaks at 530.33 eV, 531.93 eV, and 532.86 eV, which are ascribed to Fe-O, C=O, and C-O bonds, respectively [37,38]. In the Fe2p spectrum, the peaks at 707.32 eV (2p3/2) and 719.87 eV (2p1/2) are attributed to iron atoms arising from the steel ball. Peaks at 724.21 eV (2p1/2), 713.17 eV (2p3/2), and 710.81 eV (2p3/2) correspond to Fe²⁺ (2p1/2), Fe³⁺ (2p3/2), and Fe²⁺ (2p3/2), respectively, signifying that local high-temperature and high-pressure during friction lead to chemical reactions between iron in the steel balls and oxygen in the air [38,39]. Combining the O1s spectra, iron oxide films are formed for the DOAPO_Wear during friction, which are potentially composed of Fe₂O₃, FeOOH, FeO, and Fe₃O₄ [40]. In addition, the N1s spectrum of DOAPO_Wear exhibits peaks at 399.50 eV and 402.63 eV, corresponding to C-N and N-O bonds, respectively, suggesting that there are some amides turn into nitrogen oxides [41,42]. The results support that the tribofilm formed by DOAPO is composed of organic oxides and iron oxides, which would improve friction-reducing and anti-wear performance.

3.5.2. DFT Calculation

In order to reveal the influence of amide-only and amide-ester structure on the tribological properties as lubricating additives, DFT theoretical calculations of electrostatic potential (ESP) were conducted using the Gaussian16 software. Geometric optimizations were performed for both DOAPO and oleamide, applying the B3LYP hybrid exchange-correlation function. The optimized structures were characterized by harmonic vibration frequency with the minimum (Nimag = 0) or transition state (Nimag = 1) to analyze the atomic ESPs of C, H, O, and N with a 6-31G (d) basis set. The ESPs of compound molecules were calculated using Multiwfn based on the efficient algorithm, with reference to the van der Waals surface, while the molecular surface was defined as an isosurface with electron density $r = 0.001$ a.u.). Figure 8 reveals that the minimum and maximum ESP values for oleamide and DOAPO are -0.0689 , 0.0706 and -0.0656 , 0.0710 , respectively, which suggests that oleamide has stronger adsorption to metal surfaces compared to DOAPO. However, it is worth noting that DOAPO is superior to oleamide in friction-reducing and anti-wear performance, which indicates that strong adsorption does not necessarily demonstrate better tribological performance. According to the micro-IR analysis, the ester group in DOAPO is more prone to be broken than the amide group when friction occurs. It means that DOAPO could produce ester chain fractures during friction, which is more convenient to react with metal surfaces to form metal-oxide films and achieve the anti-wear effect. Meanwhile, the interfacial shear force is reduced when the ester bond is broken, which improves friction-reducing performance. In general, DOAPO can not only

form a strong adsorption film with metal surfaces through amide and ester groups but also produce chain fractures during friction to reduce interfacial shear force, improving tribological performance.

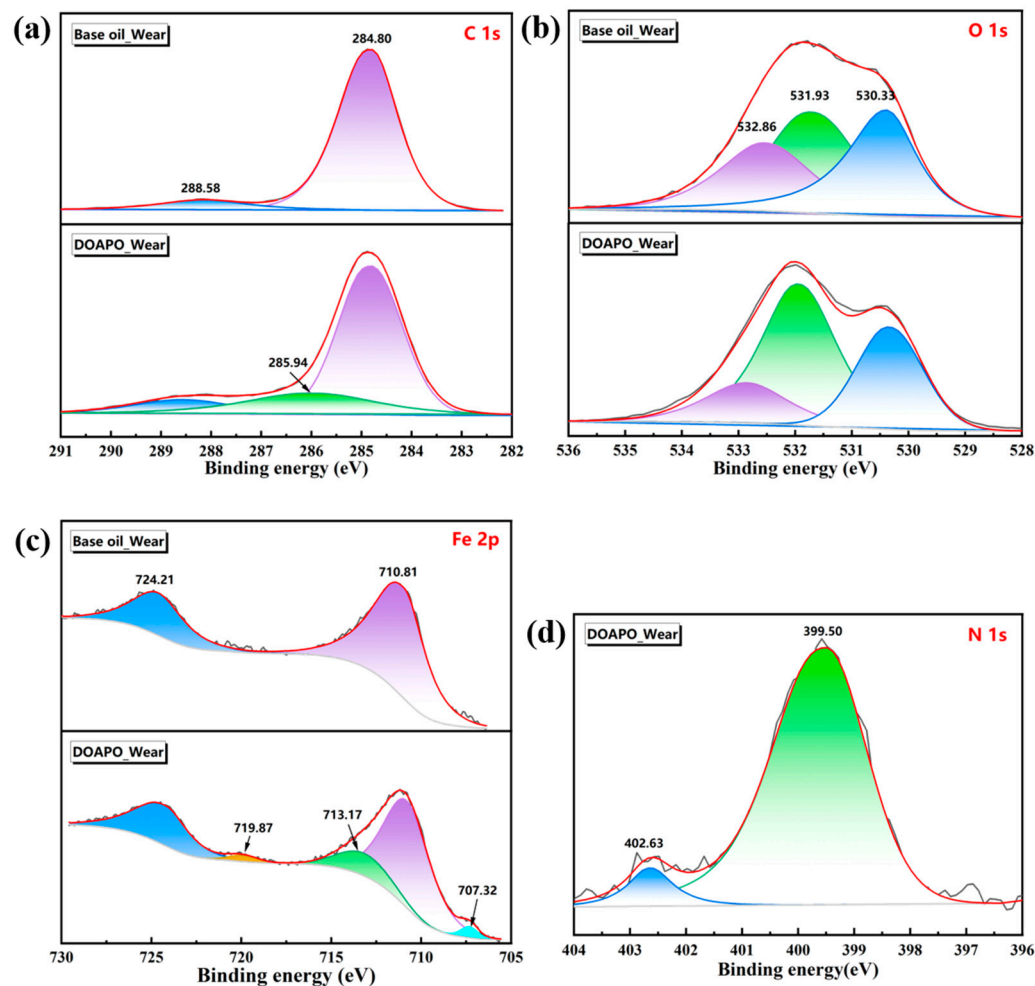


Figure 7. Worn surface analysis of base oil and oil with 0.5 wt.% DOAPO by XPS spectra: (a) C1s; (b) Fe2p; (c) O1s; (d) N1s.

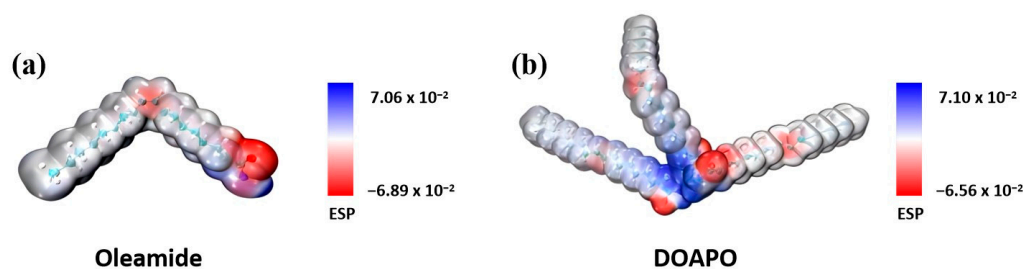


Figure 8. Theoretical electrostatic potential (ESP) calculation of (a) oleamide and (b) DOAPO.

Combining the DFT calculation and worn surface analysis, although the adsorption of DOAPO on the metal surface is slightly weaker than that of commercial oleamide (ESP: -0.0656 vs. -0.0689), ester-/amide-bonds in DOAPO are easier broken to produce polar carboxyl groups and alkyl chains during friction, as illustrated in Figure 9. While the broken chains reduce the interface shear force, and the carboxyl groups react with metal surfaces to form iron oxide protective films, so DOAPO shows good friction-reducing and anti-wear performance.

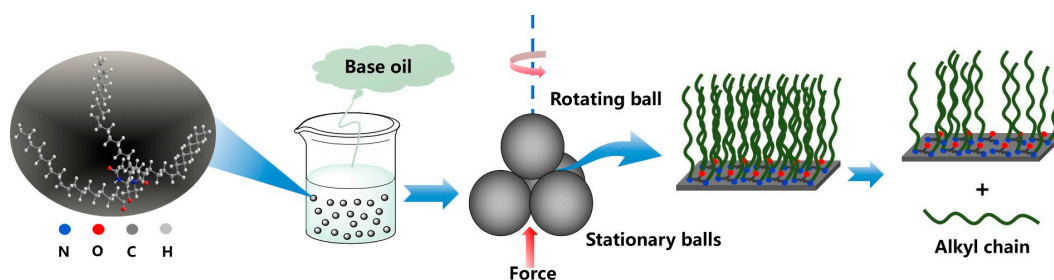


Figure 9. Schematic diagram of the lubrication mechanism with DOAPO.

4. Conclusions

In this work, a new sulfur- and phosphorus-free amide–ester, DOAPO, containing polar amide, ester, and nonpolar alkyl chains was synthesized from simple 1,3-diamino-2-propanol and OA. Its structure and thermal stability were characterized by NMR, HR-MS, FT-IR, and TGA. The tribological properties of DOAPO in synthetic base oil were studied and compared with commercial oleamide, and the micro-lubrication mechanism was disclosed by combining worn surface analysis and theoretical calculations. The following conclusions were drawn from this study:

- (1) The introduction and multi-structure of long alkyl chains make DOAPO exhibit better storage stability in synthetic base oil and better thermal stability than that of commercial oleamide, whose residual mass at 300 °C is 86.9% vs. 33.9%.
- (2) The optimal addition of DOAPO in the selected synthetic base oil is 0.5 wt.%, which can not only effectively shorten the running-in period compared to base oil (120 s vs. 600 s) but also reduce ave. COF and ave. WSD by 8.2% and 16.2%, respectively, which is better than that of commercial oleamide.
- (3) The worn surface analysis and DFT calculation show that although the adsorption of DOAPO on metal surfaces is slightly weaker than oleamide (ESP: -0.0656 vs. 0.0689), its ester bond breaks preferentially during friction, which could reduce the interfacial shear force and easily react with metal surfaces to form iron oxide films, thus demonstrating better friction-reducing and anti-wear performance.

Supplementary Materials: The following supporting information can be downloaded at <https://www.mdpi.com/article/10.3390/lubricants12060196/s1>, Figure S1: (a) ^1H NMR, (b) ^{13}C NMR, (c) HR-MS and (d) FT-IR spectra of DOAPO. Table S1: Thermal stability comparison of 1,3-diamino-2-propanol, DOAPO and oleamide. Table S2: Storage stability of oil samples with different additions of DOAPO and the same addition (0.5 wt.%) of DOAPO or oleamide. Table S3: SEM-EDS analysis of surfaces lubricated with oils before and after tribological tests. Table S4: Surface XPS analysis after friction testing of base oils and oil samples supplemented with 0.5 wt.% DOAPO.

Author Contributions: Conceptualization, H.Y., X.S. and Y.T.; methodology, H.Y. and X.S.; validation, H.Y.; formal analysis, H.Y. and X.X.; investigation, X.X. and F.Y.; calculation, Y.Z.; data curation, X.X. and F.Y.; writing—original draft preparation, H.Y. and X.X.; writing—review and editing, H.Y. and X.X.; supervision, H.Y. All authors have read and agreed to the published version of the manuscript.

Funding: This work was funded by the National Natural Science Foundation of China Joint Fund (Shanghai) project (Grant No. U23A2084) and the Ling Chuang Research Project of China National Nuclear Corporation.

Data Availability Statement: Data is contained within the article.

Conflicts of Interest: The authors declare that they have no known competing financial interests or personal relationships that could influence the work reported in this paper.

References

1. Wong, V.W.; Tung, S.C. Overview of Automotive Engine Friction and Reduction Trends—Effects of Surface, Material, and Lubricant-Additive Technologies. *Friction* **2016**, *4*, 1–28. [[CrossRef](#)]

2. McQueen, J.S.; Gao, H.; Black, E.D.; Gangopadhyay, A.K.; Jensen, R.K. Friction and Wear of Tribofilms Formed by Zinc Dialkyl Dithiophosphate Antiwear Additive in Low Viscosity Engine Oils. *Tribol. Int.* **2005**, *38*, 289–297. [[CrossRef](#)]
3. Spikes, H. Friction Modifier Additives. *Tribol. Lett.* **2015**, *60*, 5. [[CrossRef](#)]
4. Vaitkunaite, G.; Espejo, C.; Wang, C.; Thiébaud, B.; Charrin, C.; Neville, A.; Morina, A. MoS₂ Tribofilm Distribution from Low Viscosity Lubricants and Its Effect on Friction. *Tribol. Int.* **2020**, *151*, 106531. [[CrossRef](#)]
5. Hou, J.; Tsukamoto, M.; Hor, S.; Chen, X.; Yang, J.; Zhang, H.; Koga, N.; Yasuda, K.; Fukuzawa, K.; Itoh, S.; et al. Molecules with a TEMPO-Based Head Group as High-Performance Organic Friction Modifiers. *Friction* **2023**, *11*, 316–332. [[CrossRef](#)]
6. Zhou, Y.; Qu, J. Ionic Liquids as Lubricant Additives: A Review. *ACS Appl. Mater. Interfaces* **2017**, *9*, 3209–3222. [[CrossRef](#)] [[PubMed](#)]
7. Tang, Z.; Li, S. A Review of Recent Developments of Friction Modifiers for Liquid Lubricants (2007–Present). *Curr. Opin. Solid State Mater. Sci.* **2014**, *18*, 119–139. [[CrossRef](#)]
8. Meng, Y.; Xu, J.; Jin, Z.; Prakash, B.; Hu, Y. A Review of Recent Advances in Tribology. *Friction* **2020**, *8*, 221–300. [[CrossRef](#)]
9. Peeters, S.; Restuccia, P.; Loehlé, S.; Thiebaut, B.; Righi, M.C. Tribochemical Reactions of MoDTC Lubricant Additives with Iron by Quantum Mechanics/Molecular Mechanics Simulations. *J. Phys. Chem. C* **2020**, *124*, 13688–13694. [[CrossRef](#)]
10. Sarin, R.; Tuli, D.K.; Sureshbabu, A.V.; Misra, A.K.; Rai, M.M.; Bhatnagar, A.K. Molybdenum Dialkylphosphorodithioates: Synthesis and Performance Evaluation as Multifunctional Additives for Lubricants. *Tribol. Int.* **1994**, *27*, 379–386. [[CrossRef](#)]
11. Casford, M.T.L.; Puhan, D.; Davies, P.B.; Bracchi, G.L.; Smith, T.D. Thermal Behaviour of Synovene and Oleamide in Oil Adsorbed on Steel. *Tribol. Lett.* **2020**, *68*, 52. [[CrossRef](#)]
12. Shu, J.; Harris, K.; Munavirov, B.; Westbroek, R.; Leckner, J.; Glavatskih, S. Tribology of Polypropylene and Li-Complex Greases with ZDDP and MoDTC Additives. *Tribol. Int.* **2018**, *118*, 189–195. [[CrossRef](#)]
13. Tsagaropoulou, G.; Warrens, C.P.; Camp, P.J. Interactions between Friction Modifiers and Dispersants in Lubricants: The Case of Glycerol Monooleate and Polyisobutylsuccinimide-Polyamine. *ACS Appl. Mater. Interfaces* **2019**, *11*, 28359–28369. [[CrossRef](#)] [[PubMed](#)]
14. Zhang, Z.; Yamaguchi, E.S.; Kasrai, M.; Bancroft, G.M.; Liu, X.; Fleet, M.E. Tribofilms Generated from ZDDP and DDP on Steel Surfaces: Part 2, Chemistry. *Tribol. Lett.* **2005**, *19*, 221–229. [[CrossRef](#)]
15. Zhang, Z.; Yamaguchi, E.S.; Kasrai, M.; Bancroft, G.M. Tribofilms Generated from ZDDP and DDP on Steel Surfaces: Part 1, Growth, Wear and Morphology. *Tribol. Lett.* **2005**, *19*, 211–220. [[CrossRef](#)]
16. Li, W.; Kumara, C.; Meyer, H.M.; Luo, H.; Qu, J. Compatibility between Various Ionic Liquids and an Organic Friction Modifier as Lubricant Additives. *Langmuir* **2018**, *34*, 10711–10720. [[CrossRef](#)] [[PubMed](#)]
17. Ewen, J.P.; Gattinoni, C.; Morgan, N.; Spikes, H.A.; Dini, D. Nonequilibrium Molecular Dynamics Simulations of Organic Friction Modifiers Adsorbed on Iron Oxide Surfaces. *Langmuir* **2016**, *32*, 4450–4463. [[CrossRef](#)]
18. Lundgren, S.M.; Persson, K.; Mueller, G.; Kronberg, B.; Clarke, J.; Chtai, M.; Claesson, P.M. Unsaturated Fatty Acids in Alkane Solution: Adsorption to Steel Surfaces. *Langmuir* **2007**, *23*, 10598–10602. [[CrossRef](#)] [[PubMed](#)]
19. Ratoi, M.; Niste, V.B.; Alghawel, H.; Suen, Y.F.; Nelson, K. The Impact of Organic Friction Modifiers on Engine Oil Tribofilms. *RSC Adv.* **2014**, *4*, 4278–4285. [[CrossRef](#)]
20. Khatri, P.K.; Sadanandan, A.M.; Thakre, G.D.; Jain, S.L.; Singh, R.; Gupta, P. Tribo-Performance of the Ionic Liquids Derived from Dicarboxylic Acids as Lubricant Additives for Reducing Wear and Friction. *J. Mol. Liq.* **2022**, *364*, 119941. [[CrossRef](#)]
21. Campen, S.; Green, J.H.; Lamb, G.D.; Spikes, H.A. In Situ Study of Model Organic Friction Modifiers Using Liquid Cell AFM; Saturated and Mono-Unsaturated Carboxylic Acids. *Tribol. Lett.* **2015**, *57*, 18. [[CrossRef](#)]
22. Cyriac, F.; Yamashita, N.; Hirayama, T.; Yi, T.X.; Poornachary, S.K.; Chow, P.S. Mechanistic Insights into the Effect of Structural Factors on Film Formation and Tribological Performance of Organic Friction Modifiers. *Tribol. Int.* **2021**, *164*, 107243. [[CrossRef](#)]
23. Zhang, T.; Liu, S.; Zhang, X.; Gao, J.; Yu, H.; Ye, Q.; Liu, S.; Liu, W. Fabrication of Two-Dimensional Functional Covalent Organic Frameworks via the Thiol-Ene “Click” Reaction as Lubricant Additives for Antiwear and Friction Reduction. *ACS Appl. Mater. Interfaces* **2021**, *13*, 36213–36220. [[CrossRef](#)] [[PubMed](#)]
24. Kuwahara, T.; Romero, P.A.; Makowski, S.; Weihnacht, V.; Moras, G.; Moseler, M. Mechano-Chemical Decomposition of Organic Friction Modifiers with Multiple Reactive Centres Induces Superlubricity of Ta-C. *Nat. Commun.* **2019**, *10*, 151. [[CrossRef](#)] [[PubMed](#)]
25. Fry, B.M.; Chui, M.Y.; Moody, G.; Wong, J.S.S. Interactions between Organic Friction Modifier Additives. *Tribol. Int.* **2020**, *151*, 106438. [[CrossRef](#)]
26. Hu, W.; Xu, Y.; Zeng, X.; Li, J. Alkyl-Ethylene Amines as Effective Organic Friction Modifiers for the Boundary Lubrication Regime. *Langmuir* **2020**, *36*, 6716–6727. [[CrossRef](#)] [[PubMed](#)]
27. Fry, B.M.; Moody, G.; Spikes, H.A.; Wong, J.S.S. Adsorption of Organic Friction Modifier Additives. *Langmuir* **2020**, *36*, 1147–1155. [[CrossRef](#)] [[PubMed](#)]
28. Faujdar, E.; Singh, R.K. Amide Polymers Based on N-phenyl-p-phenylenediamine with α -olefins-co-maleic Anhydride as Multifunctional Additives for Lubricant Application. *Polym. Adv. Techs* **2022**, *33*, 2820–2834. [[CrossRef](#)]
29. Lee, J.; Kim, B.; Lee, J.W.; Hong, C.Y.; Kim, G.H.; Lee, S.J. Bioinspired Fatty Acid Amide-Based Slippery Oleogels for Shear-Stable Lubrication. *Adv. Sci.* **2022**, *9*, 2105528. [[CrossRef](#)]
30. Faujdar, E.; Negi, H.; Bhonsle, A.; Atray, N.; Singh, R.K. Efficiency of Dodeceny succinic Amide of n-Phenyl-p-Phenylenediamine as Novel Multifunctional Lubricant Additive for Deposit Control and Lubricity. *J. Surfactants Deterg.* **2021**, *24*, 173–184. [[CrossRef](#)]

31. Biresaw, G.; Compton, D.; Evans, K.; Bantchev, G.B. Lipoate Ester Multifunctional Lubricant Additives. *Ind. Eng. Chem. Res.* **2016**, *55*, 373–383. [[CrossRef](#)]
32. Tanaka, H.; Nagashima, T.; Sato, T.; Kawauchi, S. *The Effect of 0W-20 Low Viscosity Engine Oil on Fuel Economy*; No. 1999-01-3468; SAE International: Warrendale, PA, USA, 1999. [[CrossRef](#)]
33. *NB/SH/T 0189-2017*; Standard Test Method for Wear Preventive Characteristics of Lubricating Fluid—Four-Ball Method. National Energy Board: Beijing, China, 2017.
34. Wang, Y.; Lu, Q.; Xie, H.; Liu, S.; Ye, Q.; Zhou, F.; Liu, W. In-Situ Formation of Nitrogen Doped Microporous Carbon Nanospheres Derived from Polystyrene as Lubricant Additives for Anti-Wear and Friction Reduction. *Friction* **2023**, *12*, 439–451. [[CrossRef](#)]
35. De Barros, M.I.; Bouchet, J.; Raoult, I.; Le Mogne, T.; Martin, J.M.; Kasrai, M.; Yamada, Y. Friction Reduction by Metal Sulfides in Boundary Lubrication Studied by XPS and XANES Analyses. *Wear* **2003**, *254*, 863–870.
36. Fan, X.; Wang, L. High-Performance Lubricant Additives Based on Modified Graphene Oxide by Ionic Liquids. *J. Colloid Interface Sci.* **2015**, *452*, 98–108. [[CrossRef](#)] [[PubMed](#)]
37. Zhang, R.; Liu, X.; Guo, Z.; Cai, M.; Shi, L. Effective Sugar-Derived Organic Gelator for Three Different Types of Lubricant Oils to Improve Tribological Performance. *Friction* **2020**, *8*, 1025–1038. [[CrossRef](#)]
38. Huang, J.; Li, Y.; Jia, X.; Song, H. Preparation and Tribological Properties of Core-Shell Fe₃O₄@C Microspheres. *Tribol. Int.* **2019**, *129*, 427–435. [[CrossRef](#)]
39. Hu, J.; Zhang, Y.; Yang, G.; Gao, C.; Song, N.; Zhang, S.; Zhang, P. In-Situ Formed Carbon Based Composite Tribo-Film with Ultra-High Load Bearing Capacity. *Tribol. Int.* **2020**, *152*, 106577. [[CrossRef](#)]
40. Lee, A.Y.; Blakeslee, D.M.; Powell, C.J.; John, R.; Rumble, J. Development of the Web-Based NIST X-ray Photoelectron Spectroscopy (XPS) Database. *Data Sci. J.* **2006**, *1*, 1. [[CrossRef](#)]
41. Otero, I.; López, E.R.; Reichelt, M.; Fernández, J. Tribo-Chemical Reactions of Anion in Pyrrolidinium Salts for Steel–Steel Contact. *Tribol. Int.* **2014**, *77*, 160–170. [[CrossRef](#)]
42. Lu, Q.; Wang, H.; Ye, C.; Liu, W.; Xue, Q. Room Temperature Ionic Liquid 1-Ethyl-3-Hexylimidazolium-Bis(Trifluoromethylsulfonyl)-Imide as Lubricant for Steel–Steel Contact. *Tribol. Int.* **2004**, *37*, 547–552. [[CrossRef](#)]

Disclaimer/Publisher’s Note: The statements, opinions and data contained in all publications are solely those of the individual author(s) and contributor(s) and not of MDPI and/or the editor(s). MDPI and/or the editor(s) disclaim responsibility for any injury to people or property resulting from any ideas, methods, instructions or products referred to in the content.